Journal of Environmental Management 400 (2026) 128714

Contents lists available at ScienceDirect

Journal of Environmental Management

journal homepage: www.elsevier.com/locate/jenvman

Research article

Beyond the North-South divide: Climatic and socioeconomic interactions shape global patterns of urban greenspace exposure inequality

Yiming Zhang [a], Zhaowu Yu [a,*,1], Huiwen Zhang [a], Weiyuan Ma [a], Jinyu Hu [a], Wenjuan Ma [a], Gaoyuan Yang [b], Junga Lee [c], Yehan Wu [d]

[a] *Department of Environmental Science and Engineering, Fudan University, Shanghai, 200438, China*
[b] *School of Environmental and Geographical Sciences, Shanghai Normal University, Shanghai, China*
[c] *Division of Environmental Science and Ecological Engineering, Korea University, Seoul, 02841, Republic of Korea*
[d] *Section of Urban Design, Department of Urbanism, Faculty of Architecture and the Built Environment, Delft University of Technology, the Netherlands*

A R T I C L E I N F O

Keywords:
Greenspace exposure inequality
Global North-South
Climate zones
Socioeconomic factors
Combined impact

A B S T R A C T

Global analyses of urban greenspace have traditionally highlighted a North-South disparity, yet a critical gap remains in understanding how climatic and socioeconomic factors differentially drive greenspace exposure inequality across these regions. To address this, we introduce a novel Greenspace Exposure Inequity Index (GEII) and apply it to 1,370 cities worldwide. Our analysis reveals a more complex picture than the conventional divide: while cities in the Global South generally exhibit slightly higher inequality, those in arid regions of the Global North display greater inequity. Through a machine learning approach, we identify distinct primary drivers—the Human Development Index (HDI) dominates inequality in Global Northern cities, whereas GDP, greenspace coverage ratio (GCR), and total annual precipitation (TAP) are pivotal in the Global South. Crucially, we detect statistically significant nonlinear thresholds that act as tipping points in these relationships. Specifically, thresholds for GDP (natural-logarithm scale: 23.851) and TAP (1017.158 mm) are identified in the Global South, and for GCR (0.55) in the Global North. The identification of these thresholds provides actionable insights for urban planning: prioritizing human-centered development and equitable greening in the Global North, and optimizing greenspace planning coupled with water resource management in the Global South, to mitigate greenspace exposure inequality effectively.

1. Introduction

Urban areas, while occupying a small fraction of the Earth's land surface, are home to more than half of the global population. Although cities are engines of social and economic development, their rapid expansion has concurrently exacerbated environmental degradation and social inequities (DeFries et al., 2010; Chung et al., 2021; Wang et al., 2021; Zhao et al., 2021; Chen et al., 2025a,b). In response, green infrastructure—ranging from street trees to public parks—has been widely advocated as a cost-effective, nature-based solution to enhance urban sustainability and resilience (Kadić et al., 2025). Urban greenspaces provide a multitude of ecosystem services, including urban heat island mitigation, air purification, carbon sequestration, stormwater management, and biodiversity conservation (Kong et al., 2010; Vieira et al., 2018; Hoover and Hopton, 2019; Li and Zhou, 2019; Wang et al., 2021). Crucially, a growing body of evidence links greenspace exposure to significant human health benefits through multiple interacting pathways, including mitigation of environmental stressors, opportunities for physical activity, stress alleviation and psychological restoration, social cohesion, and enhanced perceptions of safety and well-being, ultimately contributing to reduced heat stress, lower cardiovascular morbidity, decreased obesity rates, and improved mental health and longevity (Cummins and Fagg, 2012; Kusumaning Asri et al., 2021; Maes et al., 2021; Sprague et al., 2022; Liu et al., 2023; Hardwicke et al., 2025). Acknowledging these vital functions, the World Health Organization has explicitly endorsed "universal access to greenspace" as a fundamental objective for creating healthy and livable cities (World-Health-Organization, 2017).

Despite this consensus, access to urban greenspace is profoundly unequal within and across cities (Phillips et al., 2022; Leng et al., 2023).

* Corresponding author.
E-mail address: zhaowu_yu@fudan.edu.cn (Z. Yu).
[1] Study about urban ecology, urban climate, exposure ecology, and human health.

https://doi.org/10.1016/j.jenvman.2026.128714
Received 3 December 2025; Received in revised form 7 January 2026; Accepted 20 January 2026
Available online 27 January 2026

Numerous studies have documented that affluent, low-density, or historically privileged neighborhoods often enjoy superior access to abundant, high-quality green infrastructure, whereas socioeconomically disadvantaged and densely populated communities frequently face significant greenspace deficits (Anguelovski et al., 2022; Bressane et al., 2024; Pearson et al., 2025; Sit et al., 2025). This pattern of environmental injustice, observed in contexts as diverse as the United States, Europe, China, and Brazil, translates into tangible disparities in park area and tree canopy cover (Macedo and Haddad, 2015; Nguyen et al., 2021; Song et al., 2021; Wu and Kim, 2021a,b; Anguelovski et al., 2022; Heo and Bell, 2023; Rocha et al., 2024; Winkler et al., 2024; Yu et al., 2025). Consequently, inequality in greenspace distribution can perpetuate and exacerbate underlying inequalities in mental and physical health, positioning equitable greenspace provision not merely as an environmental issue, but as a pressing matter of environmental justice and public health equity.

A primary challenge in advancing this field is the fragmented nature of existing evidence, with most studies confined to individual cities or nations and employing heterogeneous methodologies and metrics (Zhu and Cho, 2024). To overcome this limitation, recent research has begun to develop population-weighted greenspace exposure indices for global comparative analyses. For instance, Chen et al. reported a stark North-South disparity, with cities in the Global North exhibiting an average population-weighted greenspace exposure of ~45.8 %, compared to only ~14.4 % in the Global South, where inequality (as measured by the Gini coefficient) was also substantially higher (0.47 vs. 0.24) (Chen et al., 2022). Similarly, Wu et al. found that the average greenspace exposure for inhabitants of Global South cities was merely one-third of that in the Global North, with inequality approximately doubled (Wu et al., 2023). However, many assessments rely on oversimplified metrics, such as total greenspace supply or per-capita area, which can misrepresent actual human exposure to nature (Labib et al., 2020; Czesak and Różycka-Czas, 2025). These approaches often fail to capture the critical interplay between the spatial distribution of population demand and the localized availability of greenspaces in residents' immediate living environments. While robust methodologies have been applied in some regional studies, a comprehensive and standardized analysis mapping greenspace exposure inequality across a large, diverse set of global cities remains scarce, hindering a unified global understanding.

The drivers of these global disparities are similarly unclear. While several global studies have centered on a North-South divide in greenspace equality (Chen et al. 2022, 2025; Leng et al., 2023; Wu et al., 2023), this binary classification may be overly simplistic. For example, studies show that rapidly growing cities in the Global South are losing greenspace at an accelerated rate (Derdouri et al., 2025), and the proportion of urban vegetation greening is lower there than in the North (Li et al., 2025). Although this dichotomy reflects broad historical differences in development and investment, it risks obscuring the underlying heterogeneity driven by the synergistic effects of climatic and socioeconomic factors (Wu and Kim, 2021a,b). Climatic conditions—particularly precipitation and temperature—impose fundamental constraints on vegetation growth, leading to inherently lower green cover in arid and cold regions compared to humid, temperate zones (Li et al., 2024; Rao et al., 2025). Concurrently, socioeconomic development is positively correlated with greenspace provision (Chen et al., 2025a,b; Wei et al., 2025), with greenspace often treated as a “superior good” whose demand and supply increase with prosperity (Zhang et al., 2025). Yet, these two critical dimensions—climate and socioeconomic context—have not been integrated into a cohesive analytical framework to explain patterns of greenspace exposure inequality. Previous attempts, such as that of Bille et al., considered only a limited set of drivers (Bille et al., 2023), leaving a gap for a systematic global analysis that disentangles the combined and potentially differential roles of these factors in the Global North and South.

To address these knowledge gaps, this study employs our recently developed Greenspace Exposure Inequity Index (GEII) to provide a standardized assessment of inequality across 1,370 cities worldwide (Yu et al., 2023). The GEII integrates three critical dimensions: the quantity of available greenspace within a practical buffer, the distance-based accessibility to the nearest greenspace, and an equity measure (Gini index) of individual exposure levels across the population (see Methods) (Cai et al., 2025). This multi-faceted approach captures both the sufficiency of greenspace and the fairness of its distribution, offering a practical and operational metric for urban planners, as demonstrated in a pilot study in Shanghai (Yu et al., 2023). We attempt to refine existing global perspectives on greenspace exposure inequality by introducing a city-level, exposure-based metric and by systematically examining how climatic and socioeconomic factors interact within and across the Global North–South context. This research aims to answer three specific questions: (1) How do the patterns of urban greenspace exposure inequality (GEII) differ between the Global North and South? (2) What are the predominant climatic and socioeconomic drivers of GEII in Northern and Southern cities? (3) Do nonlinear response thresholds exist for the influence of these key drivers on GEII?

2. Methods

2.1. Data sources and preprocessing

2.1.1. Global urban areas

We employ the 2020 Global Urban Boundaries (GUB) shapefile, derived from a global dataset of impermeable surfaces using 30-m resolution Landsat satellite imagery (Li et al., 2020). The GUB dataset is publicly available through the project website (https://www.x-mol.com/groups/li_xuecao/dongtaizhitu). This dataset aligns closely with actual urban extents and adeptly captures the complex geometry of city boundaries, especially in peri-urban zones. However, the GUB data often splits urban areas separated by water bodies (rivers, lakes, or bays) into distinct entities. While these water bodies may hinder residents’ access to greenspaces on the opposite side, these areas typically belong to the same administrative city and share a unified urban planning and policy framework. Additionally, the dataset sometimes fragments large urban agglomerations along national borders or first-level administrative divisions. Although national boundaries represent significant administrative separations, other divisions rarely prevent residents from accessing greenspaces across them. To address this, we retain urban boundaries separated by national borders but merge those divided by water bodies or first-level administrative lines if they were within 1 km of each other. This 1 km threshold corresponds to the buffer distance used in the availability calculations. To ensure a robust sample for global analysis and exclude areas too small to qualify as cities, we apply two criteria: an area of at least 100 km^2 and a population of at least 100,000. This process yields 1,370 urban boundaries for analysis (Fig. S1). Of these, 562 cities are located in the Global North, while 808 cities are in the Global South. The Global North–South classification adopted in this study is consistent with that used by Chen et al., (2022).

2.1.2. Population

Population data are sourced from the WorldPop 2020 UN-adjusted dataset, offering 100-m resolution (Bondarenko et al., 2025). This dataset is publicly available through the WorldPop data portal (https://hub.worldpop.org/geodata/listing?id=135). It integrates multiple inputs—satellite imagery, land use, road networks, nighttime lights, building footprints, and census statistics—using machine learning to model spatial population distribution with high accuracy and detail (Stevens et al., 2015).

2.1.3. Greenspace

Greenspace data are derived from the ESA WorldCover 2020 v100 product, provided by the European Space Agency (Zanaga et al., 2021). It is publicly accessible via the ESA WorldCover repository on Zenodo (https://zenodo.org/records/5571936). This dataset, generated through multi-temporal analysis and machine learning applied to Sentinel-1 and Sentinel-2 imagery, offers a 10-m resolution global land cover classification, noted for its detail and accuracy (Venter et al., 2022). From its 11 land cover categories, we designate forests, shrubs, grasslands, herbaceous wetlands, and mangroves as greenspaces. To reduce the influence of small, isolated features (e.g., solitary trees or tiny lawns), we resample the data to 100-m resolution. For each of the 1,370 urban boundaries, we create a 1 km outward buffer, incorporating greenspace grids within this zone to mitigate potential bias near urban edges.

2.2. Index calculation

The GEII for each city is quantified by integrating population data and greenspace metrics. This methodology provides a robust and standardized metric for assessing greenspace exposure inequality, allowing for a consistent global comparison across diverse urban environments. Building on the Shanghai pilot study, we adjust Yu et al.'s approach to suit global datasets and the varied contexts of cities worldwide.

2.2.1. Availability

The availability index measures the total greenspace area within a defined radius of urban residents. We use the centroids of population and greenspace grid cells to represent residential and greenspace locations, respectively, setting a 1 km buffer radius. This distance approximates a 15-min walk, which is grounded in the "15-min city" concept, a globally adopted standard that reflects urban planning best practices for ensuring equitable access to essential services and promoting physical activity (Moreno et al., 2021; Khavarian-Garmsir et al., 2023; Zhang and Jiang, 2025). Given our reliance on raster data, calculating road network distances is impractical, so we opt for straight-line distances as a reasonable proxy.

Within each residential buffer, we compute the "distance-weighted area" of greenspaces on Google Earth Engine platform:

$$S_i = \left(1 - \frac{d_{ij}}{1000}\right) * A_j \tag{1}$$

Here, S_i is the weighted area for residential point i, d_{ij} is the distance to greenspace j, and A_j is the area of greenspace j. This linear decay function prioritizes nearer greenspaces, offering a refined measure of availability based on spatial patterns.

For each city, we normalize these weighted areas to the (0,1) range to derive the availability index:

$$I_{avi} = \frac{S_i - S_{min}}{S_{max} - S_{min}} \tag{2}$$

Where I_{avi} is the availability index, S_{min} and S_{max} denote the minimum and maximum weighted areas within the city.

2.2.2. Accessibility

The accessibility index evaluates the distance from each residential point to the nearest greenspace, calculated as:

$$D_i = min_j\left(d_{ij}\right) \tag{3}$$

Where D_i is the nearest distance for resident point i, and d_{ij} is the distance from residential point i to greenspace j. We use straight-line distances, computed in GIS, due to the limitations of raster data. Drawing on Yu et al. and recent planning standards, we normalize this distance to the (0,1) range:

$$I_{aci} = \begin{cases} 1 - \frac{D_i}{1500}, D_i < 300 \\ \frac{240}{D_i}, D_i \geq 300 \end{cases} \tag{4}$$

Where I_{aci} is the accessibility index. This piecewise approach assigns higher weights to distances under 300 m—reflecting their greater accessibility—while stabilizing the index for larger distances (Konijnendijk, 2023).

2.2.3. Gini index

The Gini index, a well-established economic measure of inequality, has gained traction in studies examining greenspace exposure (Fig. S2) (Gastwirth, 1972; Martin and Conway, 2025). It is defined as the ratio of the area between the line of equality and the Lorenz curve (Area A) to the total area under the equality line (Area A + Area B):

$$Gini = \frac{S_A}{S_A + S_B} \tag{5}$$

Since $S_A + S_B = 0.5$, this simplifies to:

$$Gini = 1 - 2^* S_B \tag{6}$$

Where B is the area under the Lorenz curve, derived via integration. Values range from 0 (perfect equality) to 1 (extreme inequality).

We calculate the Gini index for both the availability and accessibility indices across all cities. For each residential point, we compute a composite exposure index as the geometric mean of its availability and accessibility indices, tempering the influence of extreme values. The GEII for each city was then determined based on the distribution of these composite indices.

2.3. Influencing factors

We select a set of explanatory variables to examine their associations with GEII in global cities. All variables are derived from publicly available global datasets (Table S1). Natural and climatic variables include greenspace coverage ratio (GCR), total annual precipitation (TAP), and annual mean temperature (AMT). Socioeconomic variables comprise gross domestic product (GDP; taking the natural logarithm before analysis), GDP per capita (GDPpc), population density (PD), nighttime light intensity (NLI), and the Human Development Index (HDI). To improve the model's predictive capability and to capture the complex relationship between socioeconomic factors and greenspace inequality, two interaction terms are incorporated into the model. The first term, GDP/GCR, serves as an indicator of a city's economic productivity relative to its greenspace coverage, allowing us to explore how economic development within a greenspace-constrained urban environment influences GEII. This term is log-transformed to normalize its highly skewed distribution and ensure a linear relationship with the dependent variable. The second term, GDP/PD, similarly indicates whether regional economies can develop efficiently under the same population-spatial pressure, helping to reveal how concentrated economic activity interacts with greenspace inequality. These additions significantly enhanced the general performance of the model. All variables and interaction terms are harmonized to a common urban boundary and temporal reference to ensure cross-city comparability.

To quantify the combined influence of these factors on GEII, we employ the eXtreme Gradient Boosting (XGBoost), a gradient boosting decision tree algorithm, which provides a good explanation for the influencing factors of urban greenspace exposure inequality (Fig. S3). Feature importance is evaluated using the gain-based importance metric in XGBoost. It measures the average reduction in the loss function attributed to a given feature across all split nodes, reflects the overall influence of each feature on model decisions, and enables identification of the primary drivers of GEII. To further assess the direction and magnitude of individual feature effects on model predictions, we apply the Shapley Additive Explanations (SHAP) framework to decompose the model outputs into the sum of the contributions of each feature. Then, based on the SHAP dependence plots, we perform the nonlinear response analysis to determine the positive and negative contributions of the feature to GEII in different value intervals. To quantify the uncertainty of the nonlinear response thresholds, we employ the Bootstrap resampling approach (B = 500). For each resample, SHAP values are smoothed using LOESS regression, and the first negative-to-positive transition point (if uniquely present) is extracted as the response threshold (see Fig. 1).

3. Results

3.1. GEII for the Global Northern and Southern cities

3.1.1. The pattern of GEII for the Global Northern and Southern cities

Using high-resolution global population maps and land cover data, we calculate the GEII for 1,370 cities worldwide (Fig. 2). The global mean GEII was 0.493, with an average of 0.481 for the Global Northern cities (n = 562) and 0.501 for the Global Southern (n = 808), indicating marginally higher greenspace exposure inequality in the latter. Cities at higher latitudes, particularly in the Northern Hemisphere, generally exhibit lower GEII values. Conversely, some cities in certain mid-latitude and arid climates (such as Southern Europe) appear to possess a tendency toward elevated GEII values. Cities closer to the equator generally demonstrate lower GEII values, except for some regions in South America and Central Africa.

The Global North–South classification is employed in this study as a

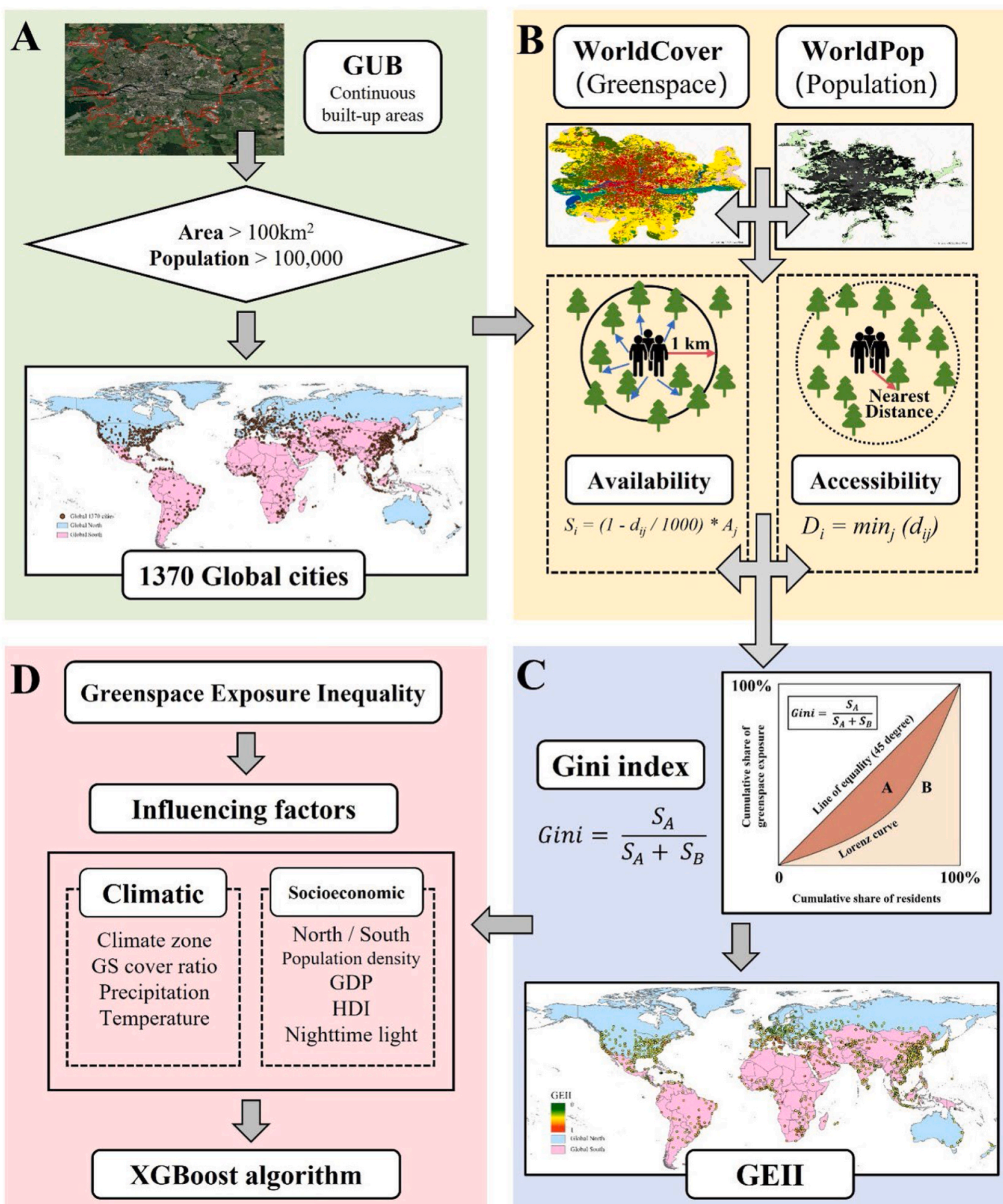

Fig. 1. Flowchart of the research with four major steps.

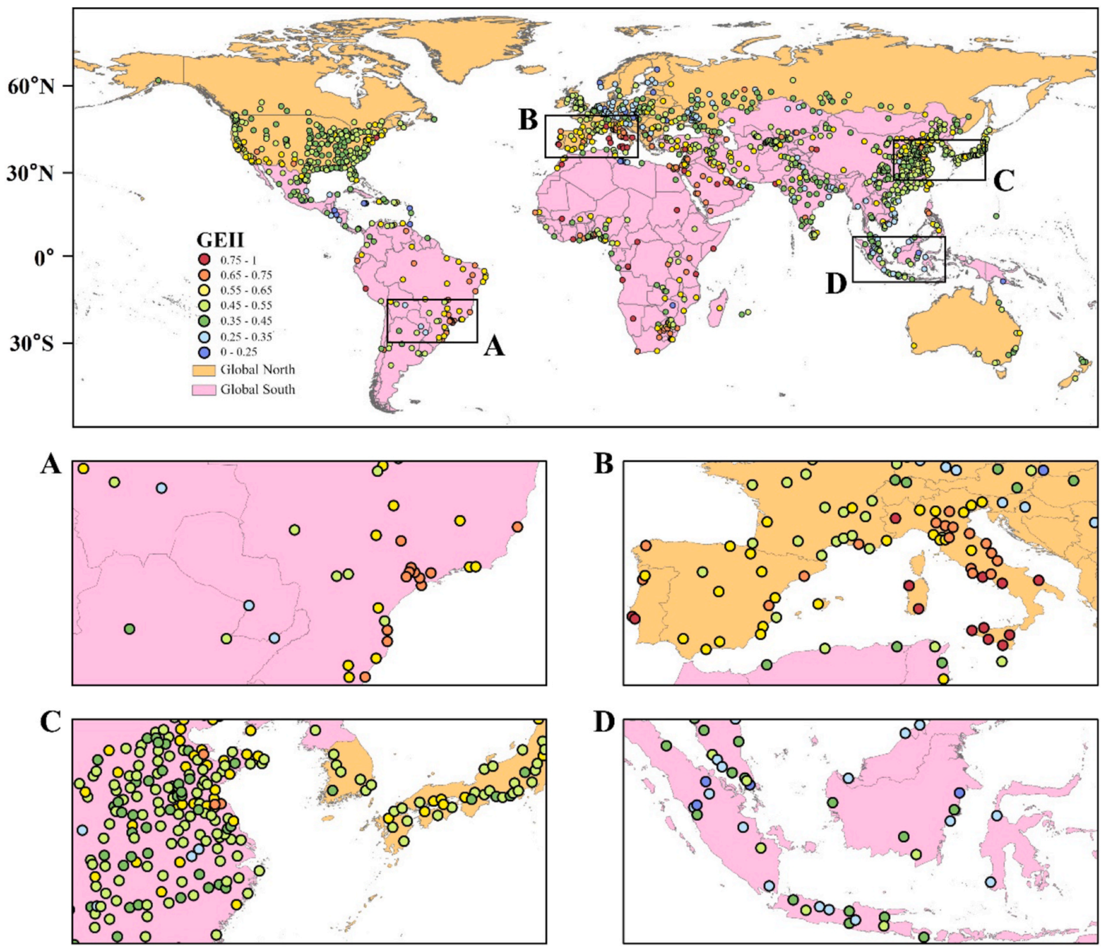

Fig. 2. Global North-South distribution pattern of GEII for 1370 cities based on the Gini index.

widely accepted proxy for broad socioeconomic differentiation among cities. Rather than serving as the sole analytical framework, it is used as a reference dimension against which the roles of climatic and other socioeconomic factors can be further examined. Accordingly, comparisons between the Global North and South are intended to reveal how additional mechanisms operate beyond this conventional divide. For example, some regional variations deviated notably from the North-South pattern, including high GEII values in Southern Europe and low values in Southeast Asia (Fig. 2). It is similarly evident in the respective patterns of availability and accessibility, both of which are relatively high in southern European cities (Fig. S4). The country-level results further highlight the presence of outliers, underscoring that national circumstances can diverge considerably from the general North–South pattern of greenspace exposure inequality. The average GEII for the ten representative countries of the Global North and the Global South (the five with the largest number of cities in the Global North and South, respectively) is: United States (0.484), Russia (0.429), Japan (0.511), Italy (0.701), and France (0.513) in the Global North; and China (0.493), India (0.426), Brazil (0.624), Mexico (0.430), and Indonesia (0.358) in the Global South. Interestingly, the average GEII values for Japan, Italy, and France in the Global North all exceed the global average, whereas those for Indonesia, India, and Mexico in the Global South fall below it.

These country-level patterns partly reflect broader regional tendencies (Fig. 2): high GEII is not only observed in Southern Europe, but also across much of South America. In contrast, relatively low GEII is found in Western and Eastern Europe as well as South Asia, while East Asia and North America remain close to the global average. Beyond these regions, cities in the Middle East and Southern Africa generally exhibit high GEII, whereas many in Western Africa display comparatively lower values.

The anomalously high GEII in Italian cities and the low GEII in Indonesian cities suggest the possible existence of other important explanatory factors for urban greenspace exposure inequality in global cities, in addition to the North-South divide. The background climate may be one of the key driving factors; however, the pronounced disparity between Indonesia and Brazil — two Global Southern countries located in the tropics — suggests that climatic classification alone cannot adequately explain the spatial pattern of GEII. Some socioeconomic factors may be equally important.

3.1.2. GEII for the Global Northern and Southern cities in different climate classifications

To investigate the influence of climate and socioeconomic development on greenspace exposure inequality, we analyze the GEII for cities categorized by the Köppen-Geiger climate classification and their affiliation with the Global North and South (Fig. 3). The result reveals that climate zones exert a more significant influence on GEII than the Global North-South divide. Among various climate categories, cities with a Mediterranean climate (Csa/Csb) exhibit the highest greenspace exposure inequality, with an average GEII of 0.584. In contrast, cities in tropical rainforest climates (Af) show the greatest equality in greenspace exposure, with an average GEII of 0.408.

On a climate-specific level, we observe nuanced differences between the Global North and South. In more humid, mid-latitude climate zones, such as continental (D) and humid temperate (Cfa/Cfb) climates, cities in the Global South generally have a slightly higher GEII than their counterparts in the Global North. Conversely, in drier climate zones, such as arid (B) and Mediterranean (Csa/Csb) climates, cities in the

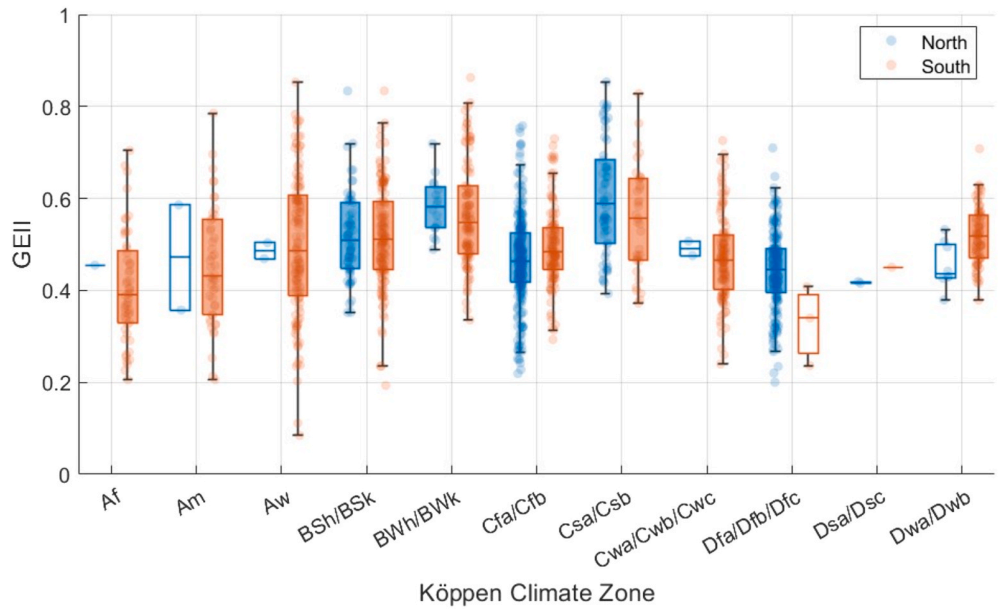

Fig. 3. GEII for the Global Northern (blue) and Southern (orange) cities within each climate classification. The climate types are named according to the Köppen-Geiger classification: Af – tropical rainforest, Am – tropical monsoon, Aw – tropical savanna, BSh/BSk – hot/cold semi-arid, BWh/BWk – hot/cold desert, Cfa/Cfb – humid subtropical/oceanic, Csa/Csb – hot-/warm-summer Mediterranean, Cwa/Cwb/Cwc – monsoon-influenced subtropical highland, Dfa/Dfb/Dfc – humid continental/subarctic, Dsa/Dsc – dry-summer continental/subarctic, and Dwa/Dwb – monsoon-influenced continental. Cities are divided into the Global North (blue) and Global South (orange). Each boxplot represents the interquartile range, with the horizontal line inside indicating the median. Scatter points represent individual city GEII values. Hollow boxplots denote categories with fewer than 10 cities.

Global North exhibit higher GEII values. Despite these variations, the average GEII difference between Global North and South cities is relatively small across most climate categories. The most substantial disparity is found within the Mediterranean climate zone, where the average GEII difference between the two groups is 0.047, far greater than the Global North-South divide (0.012). This proves that climate is a key factor affecting GEII. These results indicate that climatic classification provides an alternative and complementary lens for understanding disparities in greenspace exposure inequality. In several climate zones, the magnitude of GEII variation exceeds that observed between the Global North and South, suggesting that climate-based differentiation captures substantial heterogeneity that is obscured by a purely socioeconomic dichotomy.

3.2. *Influencing factors of the GEII for the Global Northern and Southern cities*

Based on the XGBoost model, we identify the most important factors contributing to GEII across all cities, and the Global North and South separately (Fig. 4). Our analysis reveals that HDI, TAP, and GDP/GCR are the primary determinants of GEII. While the most important factors are similar across the global and two separate models, the ranking of these factors varies significantly between the Global North and South. Specifically, for Global Northern cities, HDI and AMT are overwhelmingly the most important factors, with their significance far surpassing all others (Fig. 4B). For Global Southern cities, the most significant driver of GEII is GDP/GCR, followed by TAP and HDI. Conversely, AMT is observed to be insignificant in the Global South (Fig. 4C).

To elucidate the directional contribution of each factor to the predicted GEII, we employ SHAP values to interpret the XGBoost model. Fig. 5 visualizes these contributions for cities globally, and the Global North and South separately. The result reveals notable differences in how key factors influence GEII between the two groups. In Global Southern cities, a high TAP is consistently associated with negative SHAP values, suggesting that cities with higher precipitation tend to

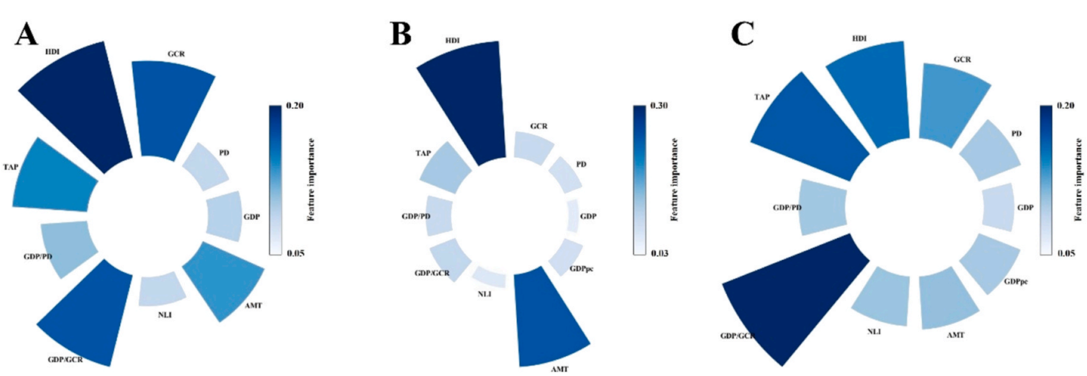

Fig. 4. Feature importance of influencing factors for global (A), Global Northern (B), and Global Southern (C) cities, calculated by the XGBoost model. The influencing factors used include: greenspace coverage ratio (GCR), total annual precipitation (TAP), annual mean temperature (AMT), gross domestic product (GDP), GDP per capita (GDPpc), population density (PD), nighttime light intensity (NLI), Human Development Index (HDI), and two interaction terms GDP/GCR and GDP/PD.

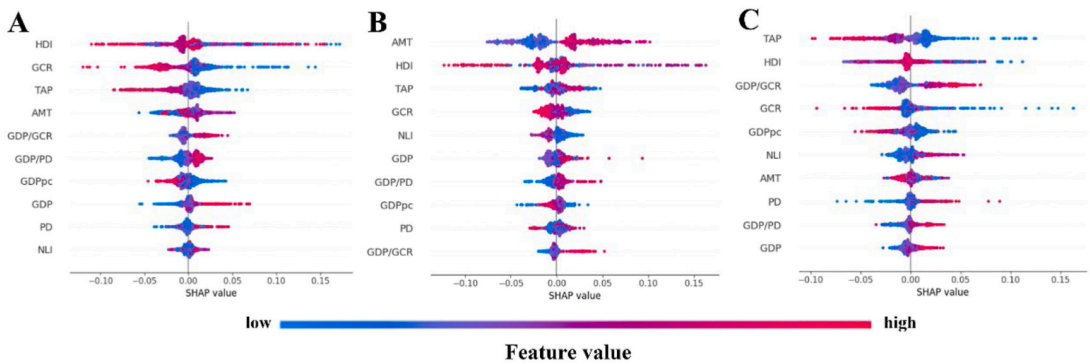

Fig. 5. Predictive contributions of various features to GEII for global (A), Global Northern (B), and Global Southern (C) cities. Each point represents an individual city value, positioned along the x-axis based on its feature's SHAP value (positive values increase GEII, while negative values decrease it). The color of each point reflects the normalized value of that city's feature, with red indicating high values and blue indicating low values.

have more equal greenspace exposure. This finding aligns with the overall global trend. However, in Global Northern cities, the influence of TAP on GEII tends to be positive, as higher precipitation is more frequently associated with greater inequality. A comparable pattern is observed with AMT: higher temperatures in Global Northern cities correspond to higher GEII values, suggesting that elevated temperatures may amplify inequalities in greenspace exposure. By contrast, this association is far weaker in Global Southern cities, where AMT does not show a consistent directional effect on GEII.

Turning to socioeconomic factors, we find a distinct North-South difference in the effect of NLI. In Global Northern cities, lower NLI values are associated with positive SHAP values, suggesting that cities with weaker nighttime illumination – and by implication lower levels of economic activity or infrastructure – tend to experience greater greenspace exposure inequality. Conversely, in Global Southern cities, higher NLI values are more often linked to positive SHAP values, indicating that in these cities, intensified economic activity and urban development are associated with greater inequality in greenspace exposure.

To further clarify how the primary influencing factors affect GEII, we perform a unidimensional feature dependency analysis on the three variables: GDP, TAP, and GCR (Fig. 6). We exclude HDI from this analysis because its limited variation within a country makes it unsuitable for this city-level differentiation. We reveal a consistent pattern for GDP across global, Northern, and Southern cities. However, the magnitude of its influence varies. Notably, the SHAP values for predominant Global Northern cities show no obvious positive or negative trend, which indicates the factor's unclear influence in this context. In Global Southern cities, we identify a clear nonlinear response threshold for GDP (taking the natural logarithm) at approximately 23.851 using the Bootstrap resampling approach (Fig. 6C). Below this threshold, SHAP values are negative, indicating that cities with lower GDP are more likely to have relatively equal greenspace exposure. And above this threshold, the SHAP values turn positive, suggesting that GDP relates to an increase in GEII. This effect will be enhanced in cities with higher AMT (Fig. S5C). Similarly, for TAP, a response threshold is identified in Global Southern cities at approximately 1017.158 mm (Fig. 6F). When TAP falls below this threshold, lower TAP corresponds to higher GEII. This effect is even more pronounced in cities with lower GDP (Fig. S5D). In contrast, Global Northern cities do not exhibit a discernible trend for this variable. The impact mechanism of GCR is similar to TAP, but the threshold appears in the Global Northern cities: when a city's GCR exceeds 0.55, its greenspace exposure tends to be more equal, mainly in the cities with lower PD (Fig. S5H). Additionally, there is a threshold for GDP/GCR in the Global South (23.307, on the

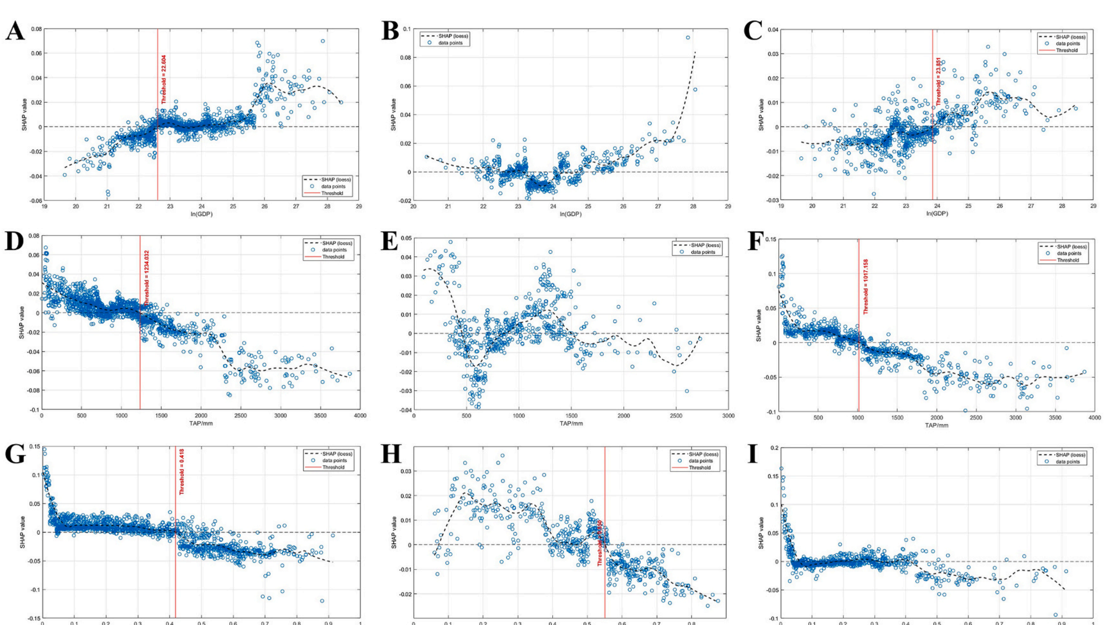

Fig. 6. SHAP unidimensional feature dependency contributions for global (A, D, G), Global Northern (B, E, H), and Global Southern (C, F, I) cities. A, B, C: the contribution of GDP. D, E, F: the contribution of TAP. G, H, I: the contribution of GCR.

natural logarithm scale, Fig. S6), suggesting the importance of integrating climate and socioeconomic factors.

4. Discussion

4.1. Interpretation of the global pattern of urban greenspace exposure inequality

The unequal distribution of urban greenspace exposure, particularly between affluent and disadvantaged communities, is a well-documented phenomenon (Chen et al. 2022, 2025; Wu et al., 2023; Rocha et al., 2024; Winkler et al., 2024). However, a comprehensive understanding of this inequality requires moving beyond a purely socioeconomic lens to incorporate the critical role of climatic constraints. Moreover, global-scale analyses that disentangle the complex interplay of these drivers have been scarce. While numerous studies have quantified greenspace disparities, many are confined to individual cities or nations and rely on disparate metrics—such as total supply (per-capita area) or simple accessibility (distance to the nearest greenspace)—that offer an incomplete picture of population exposure (Song et al., 2021; Wu and Kim, 2021a,b; Chen et al., 2022; Bille et al., 2023; Hwang et al., 2025).

We address these gaps by systematically analyzing greenspace exposure inequality across 1,370 cities spanning all major climate zones, using the population-weighted Greenspace Exposure Inequity Index (GEII). Our results suggest that urban greenspace exposure inequality should be understood as the outcome of interacting climatic and socioeconomic constraints rather than a simple manifestation of the North-South divide. While our findings confirm the general North-South disparity reported in prior research (Chen et al., 2022; Wu et al., 2023), a closer examination reveals that this divide is strongly modulated by climate. Specifically, in arid climates, cities in the Global North exhibit levels of inequality comparable to, or even exceeding, those in the Global South. It should be emphasized that this study does not aim to negate the relevance of the Global North–South divide in shaping greenspace exposure inequality, nor is it intended to replace the global North-South framework with another paradigm. On the contrary, our results confirm that this divide continues to reflect broad differences in socioeconomic development among global cities. However, by incorporating climatic variables and multiple socioeconomic indicators, we demonstrate that the Global North–South divide alone is insufficient to explain the observed spatial heterogeneity of GEII. Inequality patterns emerge from more complex and context-dependent mechanisms, in which climatic constraints and socioeconomic conditions interact and manifest differently across regions.

A key methodological advancement of this work is the application of the GEII. Unlike simpler metrics, the GEII provides a more holistic assessment by simultaneously integrating the area, proximity, and equity of greenspace distribution relative to the resident population. This rigorous quantification of actual exposure, as opposed to mere supply or accessibility, likely underpins some of the nuanced patterns observed here, which diverge from studies using less integrated indicators.

Employing ensemble machine-learning models allowed us to uniformly capture the relative importance of drivers across the global sample and, crucially, to detect nonlinear response thresholds for key variables—GDP, total annual precipitation (TAP), and greenspace coverage ratio (GCR). Our models identify distinct primary drivers in the Global North and South. In Northern cities, the Human Development Index (HDI) emerges as the dominant predictor of GEII, whereas in Southern cities, GDP, GCR, and TAP are the primary controls. These results extend previous studies by transcending the limited explanatory power of a traditional North-South dichotomy, underscoring that cities—as integrated social-ecological systems—experience greenspace inequality shaped by synergistic climatic and socioeconomic forces.

4.2. Implications of nonlinear thresholds for environmental equality and urban planning

Our findings, especially the detection of nonlinear response thresholds, have direct implications for both urban planning practice and the broader understanding of environmental justice. First, in Global Southern cities, a tipping point occurs when GDP (on a natural-logarithm scale) exceeds 23.851, beyond which further economic growth is associated with increased inequality. This suggests a growing dissonance between economic expansion and the equitable spatial allocation of greenspace benefits. In these more affluent Southern cities, planning priorities must, therefore, shift from merely expanding the total greenspace area—which may already be occurring (Fig. S7I) (Wu et al., 2023; Yu et al., 2025)—to targeted investments in greenspace provision within densely populated, underserved neighborhoods. Second, also in the Global South, we identify a precipitation threshold of 1017.158 mm, below which water scarcity exacerbates inequality. For planners in these arid cities, a dual strategy is imperative: promoting water-efficient irrigation and drought-tolerant planting to overcome bioclimatic constraints (Calderón-Argelich et al., 2021), while simultaneously dismantling socio-economic “greenspace barriers” to ensure that low-income communities are not disproportionately deprived of green amenities (Fig. S6B). Finally, in Global North cities, a GCR below 0.55 acts as a threshold that drives heightened inequality. This finding calls for an equality-driven greening agenda that combines legally binding minimum coverage targets with spatially prioritized investments in high-density, greenspace-poor districts (Figs. S6A, E, H) (Anguelovski et al., 2022).

4.3. Limitations and future research directions

Several limitations of this study should be acknowledged. First, our analysis focused on a selected set of macro-scale climatic and socioeconomic drivers. The formation of greenspace inequality is, however, a complex process influenced by more granular, place-specific factors such as community history, cultural practices, local governance capacity, land tenure systems, and detailed policy instruments. While incorporating these elements could enhance the local relevance of our models, this global-scale analysis was necessarily constrained by data availability and computational feasibility. Future research should aim to integrate these contextual drivers, particularly in Global Southern cities with prominent informal settlements, to provide a more “bottom-up” understanding of the underlying social mechanisms.

Second, our analysis adopts a uniform buffer size (1 km) to operationalize greenspace exposure across all cities. However, the effective buffer size for greenspace exposure may be spatially nonstationary. Differences in urban form, transportation infrastructure, cultural practices, and climatic conditions may lead residents in different cities to interact with greenspaces at substantially different spatial scales (Liu et al., 2024a,b). Future studies could address this limitation by incorporating adaptive or city-specific buffer schemes informed by urban morphology or empirical exposure–response relationships.

Third, this study relies on annual representations of both greenspace and population exposure, implicitly assuming temporal stationarity. In reality, both vegetation conditions and human mobility patterns can vary considerably across seasons. Ignoring temporal dynamics may introduce additional uncertainty into greenspace exposure assessments (Liu et al., 2024a,b). From a long-term perspective, the cross-sectional nature of this study, imposed by data constraints, also limits causal inference. A critical next step is to incorporate a temporal dimension to explore the long-term dynamics of GEII in response to urbanization, climate change, and policy interventions. Constructing scenario-based simulation models could help forecast future trajectories of greenspace inequality, thereby providing a robust scientific foundation for proactive and equitable urban planning.

5. Conclusion

This study extends the conventional North–South dichotomy to demonstrate that urban greenspace exposure inequality is not merely a function of geographic or economic bloc, but is critically shaped by the interplay of climatic and socioeconomic factors. While confirming the general disparity in greenspace exposure between the Global North and South, our analysis of 1,370 cities reveals that this binary framework is insufficient. We show that climatic conditions are a constitutive force in shaping inequality, to the extent that they can invert the expected North–South pattern in specific contexts, such as in arid regions.

Central to this refined understanding is the application of the GEII, which advances upon previous metrics by integrating availability, accessibility, and equity at the population level. This approach overcomes the limitations of supply- or distance-based measures, providing a standardized and demographically sensitive assessment of exposure. By integrating high-resolution spatial data with explainable machine learning, we further identified distinct primary drivers in each hemisphere: socioeconomic development (HDI) in the Global North, and a combination of economic capacity (GDP), existing greenspace coverage (GCR), and precipitation (TAP) in the Global South.

A key and novel contribution of this work is the discovery of statistically significant nonlinear thresholds in these drivers. The identification of specific tipping points for GDP (ln-transformed: 23.851) and annual precipitation (1017.158 mm) in the Global South, and for greenspace coverage (GCR: 0.55) in the Global North, provides a quantitative foundation for targeted policy intervention. These thresholds, previously unmapped at a global scale, offer a more nuanced and operational lens for understanding urban greening processes, suggesting that the relationship between development and equity is not linear but can shift fundamentally once critical points are reached. Consequently, our findings provide a more nuanced and actionable framework for tackling urban environmental inequality, emphasizing that effective strategies must be tailored to a city's specific climatic and socioeconomic context.

CRediT authorship contribution statement

Yiming Zhang: Writing – original draft, Visualization, Validation, Methodology, Formal analysis, Data curation, Conceptualization. **Zhaowu Yu:** Writing – review & editing, Supervision, Project administration. **Huiwen Zhang:** Writing – review & editing, Supervision. **Weiyuan Ma:** Writing – review & editing, Methodology, Conceptualization. **Jinyu Hu:** Writing – review & editing, Data curation. **Wenjuan Ma:** Writing – review & editing. **Gaoyuan Yang:** Writing – review & editing. **Junga Lee:** Writing – review & editing. **Yehan Wu:** Writing – review & editing.

Declaration of competing interest

All authors have approved this manuscript and declare no competing interests. This manuscript is original, has not been published before, and is not currently under consideration elsewhere.

Acknowledgments

This atudy was supported by the National Science Foundation of China (Grant no. 42401103); National Key R&D Program of China (Grant no. 2024YFF130700).

Appendix A. Supplementary data

Supplementary data to this article can be found online at https://doi.org/10.1016/j.jenvman.2026.128714.

Data availability

Data will be made available on request.

References

Anguelovski, I., Connolly, J.J.T., Cole, H., Garcia-Lamarca, M., Triguero-Mas, M., Baró, F., Martin, N., Conesa, D., Shokry, G., del Pulgar, C.P., Ramos, L.A., Matheney, A., Gallez, E., Oscilowicz, E., Máñez, J.L., Sarzo, B., Beltrán, M.A., Minaya, J.M., 2022. Green gentrification in European and North American cities. Nat. Commun. 13, 3816.

Bille, R.A., Jensen, K.E., Buitenwerf, R., 2023. Global patterns in urban green space are strongly linked to human development and population density. Urban For. Urban Green. 86, 127980.

Bondarenko, M., Priyatikanto, R., Tejedor-Garavito, N., Zhang, W., McKeen, T., Cunningham, A., Woods, T., Hilton, J., Cihan, D., Nosatiuk, B., Brinkhoff, T., Tatem, A., Sorichetta, A., 2025. Constrained estimates of 2015-2030 total number of people per grid square at a resolution of 3 arc (approximately 100m at the equator) R2025A version v1. Global Demographic Data Project - Funded by The Bill and Melinda Gates Foundation (INV-045237). WorldPop. School of Geography and Environmental Science, University of Southampton.

Bressane, A., Loureiro, A.I., Negri, R.G., 2024. Environmental racism in the accessibility of urban green space: a case study of a metropolitan area in an emerging economy. Urban Sci. 8, 224.

Cai, W., Zhang, C., Zhang, S., Bai, Y., Chen, B., Chen, J., Cheng, L., Fan, W., Feng, L., Guan, D., Hong, C., Hu, Y., Hua, J., Huang, C., Huang, H., Huang, J., Huang, X., Ji, J. S., Jiang, Q., Jiang, X., Kan, H., Kang, J., Kiesewetter, G., Li, B., Li, G., Li, T., Liao, W., Lin, B., Lin, H., Liu, H., Liu, Q., Liu, X., Liu, Y., Liu, Z., Liu, Z., Liu, Z., Lou, S., Lu, B., Lu, C., Ma, W., Mi, Z., Miao, Y., Mo, G., Repke, T., Ren, C., Romanello, M., Shen, J., Su, J., Su, R., Sun, Y., Tang, X., Walawender, M., Wang, C., Wang, H., Wang, Q., Wang, Q., Wang, Y., Wei, W., Wen, S., Xiong, H., Xu, B., Yang, X., Yang, Y., Yao, F., Yin, M., Yu, L., Yu, Z., Zhang, J., Zhang, R., Zhang, S., Zhang, S., Zhang, Z., Zhao, M., Zhao, Q., Zheng, D., Zhou, H., Zhou, J., Zhou, Y., Luo, Y., Gong, P., 2025. The 2025 China report of the lancet countdown on health and climate change: empowering cities for synergistic action. Lancet Public Health.

Calderón-Argelich, A., Benetti, S., Anguelovski, I., Connolly, J.J.T., Langemeyer, J., Baró, F., 2021. Tracing and building up environmental justice considerations in the urban ecosystem service literature: a systematic review. Landsc. Urban Plann. 214, 104130.

Chen, B., Wu, S., Song, Y., Webster, C., Xu, B., Gong, P., 2022. Contrasting inequality in human exposure to greenspace between cities of Global North and Global South. Nat. Commun. 13, 4636.

Chen, J., Li, H., Luo, S., Su, D., Zang, T., Kinoshita, T., Yang, L., 2025a. How do economic levels, urbanization, and infrastructure investments influence inequality in urban green space exposure? Insights from Japanese municipalities. Urban For. Urban Green. 104, 128649.

Chen, J., Qiu, B., Chakraborty, T.C., Miao, X., Cao, Y., Li, L., Zhao, S., Ni, Y., Tian, X., Qian, Y., Guo, W., 2025b. Contrasting effects of urbanization on vegetation between the Global South and Global North. Nat. Sustain. 8, 373–384.

Chung, M.G., Frank, K.A., Pokhrel, Y., Dietz, T., Liu, J., 2021. Natural infrastructure in sustaining global urban freshwater ecosystem services. Nat. Sustain. 4, 1068–1075.

Cummins, S., Fagg, J., 2012. Does greener mean thinner? Associations between neighbourhood greenspace and weight status among adults in England. Int. J. Obes. 36, 1108–1113.

Czesak, B., Różycka-Czas, R., 2025. Assessing accessibility and crowding in urban green spaces: a comparative study of approaches. Landsc. Urban Plann. 257, 105301.

DeFries, R.S., Rudel, T., Uriarte, M., Hansen, M., 2010. Deforestation driven by urban population growth and agricultural trade in the twenty-first century. Nat. Geosci. 3, 178–181.

Derdouri, A., Murayama, Y., Morimoto, T., Wang, R., Haji Mirza Aghasi, N., 2025. Urban green space in transition: a cross-continental perspective from eight Global North and South cities. Landsc. Urban Plann. 253, 105220.

Gastwirth, J.L., 1972. The estimation of the lorenz curve and gini index. Rev. Econ. Stat. 54, 306–316.

Hardwicke, J., Hill, K.M., Ryan, D.J., 2025. The significance of urban greenspaces in everyday life. Int. Rev. Sociol. 35, 48–71.

Heo, S., Bell, M.L., 2023. Investigation on urban greenspace in relation to sociodemographic factors and health inequity based on different greenspace metrics in 3 US urban communities. J. Expo. Sci. Environ. Epidemiol. 33, 218–228.

Hoover, F.-A., Hopton, M.E., 2019. Developing a framework for stormwater management: leveraging ancillary benefits from urban greenspace. Urban Ecosyst. 22, 1139–1148.

Hwang, B., Ko, C., Im, D., Kang, W., 2025. Network-based assessment of urban forest and green space accessibility in six major cities: london, New York, Paris, Tokyo, Seoul, and Beijing. Urban For. Urban Green. 107, 128781.

Kadić, A., Maljković, B., Rogulj, K., Pamuković, J.K., 2025. Green infrastructure's role in climate change adaptation: summarizing the existing research in the Most benefited policy sectors. Sustainability 17, 4178.

Khavarian-Garmsir, A.R., Sharifi, A., Sadeghi, A., 2023. The 15-minute city: urban planning and design efforts toward creating sustainable neighborhoods. Cities 132, 104101.

Kong, F., Yin, H., Nakagoshi, N., Zong, Y., 2010. Urban green space network development for biodiversity conservation: identification based on graph theory and gravity modeling. Landsc. Urban Plann. 95, 16–27.

Konijnendijk, C.C., 2023. Evidence-based guidelines for greener, healthier, more resilient neighbourhoods: introducing the 3–30–300 rule. J. For. Res. 34, 821–830.

Kusumaning Asri, A., Lee, H.-Y., Pan, W.-C., Tsai, H.-J., Chang, H.-T., Candice Lung, S.-C., Su, H.-J., Yu, C.-P., Ji, J.S., Wu, C.-D., Spengler, J.D., 2021. Is green space exposure beneficial in a developing country? Landsc. Urban Plann. 215, 104226.

Labib, S.M., Shuvo, F.K., Browning, M.H.E.M., Rigolon, A., 2020. Noncommunicable diseases, park prescriptions, and urban green space use patterns in a global south context: the case of Dhaka, Bangladesh. Int. J. Environ. Res. Publ. Health 17, 3900.

Leng, S., Sun, R., Yang, X., Chen, L., 2023. Global inequities in population exposure to urban greenspaces increased amidst tree and nontree vegetation cover expansion. Commun. Earth Environ. 4, 464.

Li, G., Cao, Y., Fang, C., Sun, S., Qi, W., Wang, Z., He, S., Yang, Z., 2025. Global urban greening and its implication for urban heat mitigation. Proc. Natl. Acad. Sci. USA 122, e2417179122.

Li, X., Gong, P., Zhou, Y., Wang, J., Bai, Y., Chen, B., Hu, T., Xiao, Y., Xu, B., Yang, J., Liu, X., Cai, W., Huang, H., Wu, T., Wang, X., Lin, P., Li, X., Chen, J., He, C., Li, X., Yu, L., Clinton, N., Zhu, Z., 2020. Mapping global urban boundaries from the global artificial impervious area (GAIA) data. Environ. Res. Lett. 15, 094044.

Li, X., Zhou, W., 2019. Optimizing urban greenspace spatial pattern to mitigate urban heat island effects: extending understanding from local to the city scale. Urban For. Urban Green. 41, 255–263.

Li, Y., Svenning, J.C., Zhou, W., Zhu, K., Abrams, J.F., Lenton, T.M., Ripple, W.J., Yu, Z., Teng, S.N., Dunn, R.R., Xu, C., 2024. Green spaces provide substantial but unequal urban cooling globally. Nat. Commun. 15, 7108.

Liu, Y., Kwan, M.-P., Wang, J., 2024a. Analytically articulating the effect of buffer size on urban green space exposure measures. Int. J. Geogr. Inf. Sci. 39, 255–276.

Liu, Y., Kwan, M.-P., Yu, C., 2024b. How mobility and temporal contexts may affect environmental exposure measurements: using outdoor artificial light at night (ALAN) and urban green space as examples. Ann. Assoc. Am. Geogr. 114, 1098–1117.

Liu, Y., Kwan, M.P., Wong, M.S., Yu, C., 2023. Current methods for evaluating people's exposure to green space: a scoping review. Soc. Sci. Med. 338, 116303.

Macedo, J., Haddad, M.A., 2015. Equitable distribution of open space: using spatial analysis to evaluate urban parks in Curitiba, Brazil. Environ. Plann. Plann. Des. 43, 1096–1117.

Maes, M.J.A., Pirani, M., Booth, E.R., Shen, C., Milligan, B., Jones, K.E., Toledano, M.B., 2021. Benefit of woodland and other natural environments for adolescents' cognition and mental health. Nat. Sustain. 4, 851–858.

Martin, A.J.F., Conway, T.M., 2025. Using the gini index to quantify urban green inequality: a systematic review and recommended reporting standards. Landsc. Urban Plann. 254, 105231.

Moreno, C., Allam, Z., Chabaud, D., Gall, C., Pratlong, F., 2021. Introducing the "15-Minute city": sustainability, resilience and place identity in future post-pandemic cities. Smart Cities 4, 93–111.

Nguyen, P.Y., Astell-Burt, T., Rahimi-Ardabili, H., Feng, X., 2021. Green space quality and health: a systematic review. Int. J. Environ. Res. Publ. Health 18, 11028.

Pearson, A.L., Reuben, A., Roberts, J.D., Beyer, K.M.M., Browning, M.H.E.M., Lin, Z., Hartig, T., 2025. Greenspace will not always disproportionately benefit disadvantaged urban residents. Nature Cities 2, 489–495.

Phillips, A., Canters, F., Khan, A.Z., 2022. Analyzing spatial inequalities in use and experience of urban green spaces. Urban For. Urban Green. 74, 127674.

Rao, P., Torreggiani, D., Tassinari, P., Rötzer, T., Pauleit, S., Rahman, M.A., 2025. Do urban green spaces cool cities differently across latitudes? Spatial variability and climatic drivers of vegetation-induced cooling. Sustain. Cities Soc. 130, 106513.

Rocha, A.D., Vulova, S., Förster, M., Gioli, B., Matthews, B., Helfter, C., Meier, F., Steeneveld, G.-J., Barlow, J.F., Järvi, L., Chrysoulakis, N., Nicolini, G., Kleinschmit, B., 2024. Unprivileged groups are less served by green cooling services in major European urban areas. Nature Cities 1, 424–435.

Sit, K.Y., Chen, W.Y., Ng, K.Y., Koh, K., Zhang, H., 2025. Unveiling environmental inequalities in high-density Asian city: city-scaled comparative analysis of green space coverage within 10-minute walk from private, public, and rural housing. Landsc. Urban Plann. 253, 105225.

Song, Y., Chen, B., Ho, H.C., Kwan, M.-P., Liu, D., Wang, F., Wang, J., Cai, J., Li, X., Xu, Y., He, Q., Wang, H., Xu, Q., Song, Y., 2021. Observed inequality in urban greenspace exposure in China. Environ. Int. 156, 106778.

Sprague, N.L., Bancalari, P., Karim, W., Siddiq, S., 2022. Growing up green: a systematic review of the influence of greenspace on youth development and health outcomes. J. Expo. Sci. Environ. Epidemiol. 32, 660–681.

Stevens, F.R., Gaughan, A.E., Linard, C., Tatem, A.J., 2015. Disaggregating census data for population mapping using random forests with remotely-sensed and ancillary data. PLoS One 10, e0107042.

Venter, Z.S., Barton, D.N., Chakraborty, T., Simensen, T., Singh, G., 2022. Global 10 m land use land cover datasets: a comparison of dynamic world, world cover and esri land cover. Remote Sens. 14, 4101.

Vieira, J., Matos, P., Mexia, T., Silva, P., Lopes, N., Freitas, C., Correia, O., Santos-Reis, M., Branquinho, C., Pinho, P., 2018. Green spaces are not all the same for the provision of air purification and climate regulation services: the case of urban parks. Environ. Res. 160, 306–313.

Wang, J., Chen, Y., Liao, W., He, G., Tett, S.F.B., Yan, Z., Zhai, P., Feng, J., Ma, W., Huang, C., Hu, Y., 2021. Anthropogenic emissions and urbanization increase risk of compound hot extremes in cities. Nat. Clim. Change 11, 1084–1089.

Wang, Y., Chang, Q., Li, X., 2021. Promoting sustainable carbon sequestration of plants in urban greenspace by planting design: a case study in parks of Beijing. Urban For. Urban Green. 64, 127291.

Wei, L., Liu, Z., Zhou, Y., Tao, Z., Yang, F., 2025. Global urban green spaces in the functional urban areas: spatial pattern, drivers and size hierarchy. Urban For. Urban Green. 107, 128770.

Winkler, R.L., Clark, J.A.G., Locke, D.H., Kremer, P., Aronson, M.F.J., Hoover, F.-A., Joo, H.E., La Rosa, D., Lee, K.J., Lerman, S.B., Pearsall, H., Vargo, T.L.V., Nilon, C.H., Lepczyk, C.A., 2024. Unequal access to social, environmental and health amenities in US urban parks. Nature Cities 1, 861–870.

World-Health-Organization, 2017. Shanghai consensus on healthy cities 2016. Health Promot. Int. 32, 603–605.

Wu, L., Kim, S.K., 2021a. Does socioeconomic development lead to more equal distribution of green space? Evidence from Chinese cities. Sci. Total Environ. 757, 143780.

Wu, L., Kim, S.K., 2021b. Exploring the equality of accessing urban green spaces: a comparative study of 341 Chinese cities. Ecol. Indic. 121, 107080.

Wu, S., Chen, B., Webster, C., Xu, B., Gong, P., 2023. Improved human greenspace exposure equality during 21st century urbanization. Nat. Commun. 14, 6460.

Yu, Z., Ma, W., Hu, J., Yang, G., Liu, H., Zhou, Y., Li, X., Li, Y., Guan, C., Ma, W., Hu, Y., Zhang, Y., Yang, W., Jiang, B., Zhou, W., 2025. Greening dominates greenspace exposure inequality in Chinese cities. npj Urban Sustainability 5, 73.

Yu, Z., Ma, W., Hu, S., Yao, X., Yang, G., Yu, Z., Jiang, B., 2023. A simple but actionable metric for assessing inequity in resident greenspace exposure. Ecol. Indic. 153, 110423.

Zhang, B., Jiang, T., 2025. Seasonal disparities in green exposure under the 15-minute city framework: a case study of Xi`an, China. Sci. Rep. 15, 28166.

Zhang, H.-L., Wang, W., Wang, Y., Meng, F., Shi, R., Xue, H., Nizamani, M.M., Zhao, Z., 2025. Socio-economic drivers and sustainability challenges of urban green space distribution in Jinan, China. Sustainability 17, 5993.

Zhao, L., Oleson, K., Bou-Zeid, E., Krayenhoff, E.S., Bray, A., Zhu, Q., Zheng, Z., Chen, C., Oppenheimer, M., 2021. Global multi-model projections of local urban climates. Nat. Clim. Change 11, 152–157.

Zhu, Z., Cho, D.-g., 2024. Urban green space research progress and hotspots evolution analysis: visual analysis based on WOS. Journal of People, Plants, and Environment 27, 69–78.

Zanaga, D., Van De Kerchove, R., De Keersmaecker, W., Souverijns, N., Brockmann, C., Quast, R., Wevers, J., Grosu, A., Paccini, A., Vergnaud, S., Cartus, O., Santoro, M., Fritz, S., Georgieva, I., Lesiv, M., Carter, S., Herold, M., Li, Linlin, Tsendbazar, N.E., Ramoino, F., Arino, O., 2021. ESA WorldCover 10 m 2020 v100.